

# Original Research

## Identification of histone acetylation in a murine model of allergic asthma by proteomic analysis

Yuan Ren, Menglu Li, Shiyao Bai, Lingfei Kong and Xinming Su 

Department of Pulmonary and Critical Care Medicine, Institute of Respiratory Diseases, The First Affiliated Hospital of China Medical University, Shenyang 110001, P.R. China

Corresponding author: Xinming Su. Email: xinming\_med@126.com/SUxm123@hotmail.com

### Impact statement

The specific sites of histone acetylation modification in pathogenesis of asthma remain indistinct. For the first time, our study identified 15 potential differentially expressed histone acetylation sites associated with asthma and explored the distribution of the identified histone acetylation sites in cells involved in asthma pathogenesis using isobaric tag for relative and absolute quantization (iTRAQ) combined with liquid chromatography tandem-mass spectrometry (LC-MS/MS). The results revealed that histone acetylation modification in asthma occurred mainly in H2B and H3 rather than other histones; and the expressions of these identified acetylation sites were distributed differentially in asthmatic lung tissue according to cell types. Our findings may provide scientific base in the development of specific epigenetic modifying agents for asthma treatment.

### Abstract

The pathogenesis of asthma is closely related to histone acetylation modification, but the specific acetylation sites related to this process remain indistinct. Herein, our study sought to identify differentially modified acetylation sites and their expression distribution in cells involved in asthma in lung tissues. The airway hyper-responsiveness, inflammation, and remodeling were assessed by non-invasive whole-body plethysmography, ELISA, and hematoxylin-eosin staining to confirm the successful establishment of the allergic asthma model. Afterward, the differentially modified acetylation sites in asthmatic lung tissues were identified and validated by using proteomics and western blotting, respectively. The immunohistochemistry analysis was applied to reveal the distribution of identified acetylation sites in asthmatic lung tissues. A total of 15 differentially modified acetylation sites, including 13 upregulated (H3K9ac, H3K14ac, H3K18ac, H3K23ac, H3K27ac, H3K36ac, H2B1KK120ac, H2B2BK20ac, H2BK16ac, H2BK20ac, H2BK108ac, H2BK116ac, and H2BK120ac) and 2 downregulated (H2BK5ac and H2BK11ac) sites were identified and validated. Furthermore, immunohistochemical staining of lung tissues showed that nine of the identified histone acetylation sites (H2BK5, H2BK11, H3K18, H2BK116, H2BK20, H2BK120, H3K9, H3K36, and H3K27) were differentially expressed in airway epithelial

cells, and the acetylation of identified H3 histones were observed in both eosinophil and perivascular inflammatory cells. Additionally, differential expression of histone acetylation sites was also observed in nucleus of airway epithelial cells, vascular smooth muscle cells, perivascular inflammatory cells, and airway smooth muscle cells. In conclusion, we identified potential acetylation sites associated with asthma pathogenesis. These findings may contribute greatly in the search for therapeutic approaches for allergic asthma.

**Keywords:** Bronchial asthma, histone acetylation, proteomics, tandem mass tag

*Experimental Biology and Medicine* 2021; 246: 929–939. DOI: 10.1177/1535370220980345

### Introduction

As an inflammatory disease of the airways, asthma has the attributes of airway hyperresponsiveness and inflammation and affects around 300 million people worldwide.<sup>1</sup> Although a number of clinical and biological asthma phenotypes have been described, the pathogenesis of asthma remains elusive. Chromatin modification is the addition or removal of chemical groups from the components of chromosomes including DNA, RNA, histones, and non-histones, which change the structure of the chromatin

and regulate gene expression.<sup>2</sup> In the past few decades, numerous studies have shown that gene expression in asthmatic inflammation is closely related to histone modifications including acetylation, methylation, and succinylation.<sup>3</sup> Among them, acetylation plays a regulatory role in the transcription activation process of inflammatory genes.<sup>4–6</sup> Histone acetylation often happens at the lysine residues and is regulated by histone acetyltransferases, which could be reversed by histone deacetylases (HDACs).<sup>7</sup> Multiple studies have demonstrated that the

use of HDAC inhibitors can significantly alleviate related symptoms including asthmatic airway inflammation, airway hyper-responsiveness, as well as airway remodeling.<sup>8–11</sup> A research conducted by Stefanowicz *et al.* indicated that the acetylation level of H3K18 in the airway epithelium from asthmatic subjects was obviously higher than that in normal subjects.<sup>12</sup> Seumois *et al.* suggested that enhancer profiling for histone H3Lys4 dimethyl (H3K4me2) could be used for studying the functions of specialized cell types involved in asthma pathogenesis.<sup>13</sup> TGF- $\beta$ 1 is a cytokine which is involved in several cellular functions and may cause the cells to undergo epithelial mesenchymal transitions (EMT). Increasing evidence showed that EMT inducers interact with TGF- $\beta$ 1 in different ways to participate in the pathogenesis of lung diseases including asthma.<sup>14</sup> Additionally, Lee *et al.* confirmed that high acetylation level of histones (H3 and H4) is closely related to high expression of TGF- $\beta$ 1, and high secretion level of TGF- $\beta$ 1 in the airway is directly involved in asthma pathogenesis.<sup>15</sup> However, the underlying mechanism of histone acetylation regulating asthma pathogenesis remains elusive.

As one of the widely employed techniques in proteomics, the derivatization of peptides with isobaric tags has gained popularity in the last decade, which included iTRAQ and tandem mass tag (TMT).<sup>16,17</sup> As a chemical labeling method, TMT labeling applies isobaric mass labels to accurately quantify and identify biological macromolecules based on mass spectrometry. Several studies demonstrated that TMT labeling could improve sensitivity and save time in large-scale proteomics studies.<sup>18</sup>

It is known that the pathogenesis of asthma is closely related to histone acetylation modification, but the specific acetylation sites related to this process are not fully identified. In this study, we sought to identify the differentially modified acetylation sites between the lung tissue from healthy and allergic asthma mice by combination of TMT labeling method and the technique of tandem mass spectrometry. Additionally, we detected the identified acetylation sites in lung tissues of healthy and allergic asthma mice by using immunohistochemical (IHC) staining to provide scientific base for further exploration of the underlying mechanism of histone acetylation in asthma pathogenesis.

## Materials and methods

### Establishment and grouping of animal models

Twenty-four female BALB/C mice which were 6–8 weeks old were accommodated in an SPF grade room with humidity of 40%–60% and temperature of  $22 \pm 2^\circ\text{C}$ . Food and water were freely accessible to mice. Mice were randomly distributed into two groups (a normal control group and a model group with 12 mice in each group) without significant age difference by using the random number table. The selection of sample size in each group was performed as previously described.<sup>19</sup> Initially, the mice of model group were administrated with 20  $\mu\text{g}$  of ovalbumin

(OVA) in an intraperitoneal injection way. As previously reported,<sup>11</sup> 4 mg/ml of aluminum hydroxide gel was used to intraperitoneally administrate the mice on days 0, 7, and 14 for sensitization. For mice from the normal control group, OVA was replaced by normal saline. A week after the last sensitization, the mice were subjected to OVA atomization by using an ultrasonic atomizing device. The atomization scheme was as follows: OVA concentration (20 mg/ml); inhaling 3 ml/min for half an hour in each atomization; three times/week for 8 weeks. All procedures regarding animal experiments were approved by the Institutional Animal Care and Use Committee of The First Affiliated Hospital of China Medical University.

### Detection of airway responsiveness in mice

As stated before,<sup>11</sup> 24 h after excitation, airway resistance was examined by using non-invasive whole-body plethysmography to evaluate pulmonary function (Emka technologies, Paris, France). To evaluate airway resistance, enhanced pause (Penh) was recorded 3 min after administration with different concentrations of acetyl- $\beta$ -methylcholine chloride (0, 3.125, 6.25, 12.5, 25, and 50 mg/ml) (Sigma, USA). The mathematical formulae were  $\text{Penh} = \text{PEP} / \text{PIP} \times \text{Pause}$  and  $\text{Enhanced Pause} = (\text{Te} - \text{Tr}) / \text{Tr}$  wherein  $\text{PEP}$  = Peak Expiration Pressure (mL/s),  $\text{PIP}$  = Peak Inspiration Pressure (mL/s),  $\text{Te}$  = Expiratory time (s), and  $\text{Tr}$  = Relaxation time (s).

### Bronchoalveolar lavage fluid collection and measurement

After evaluating the lung function, bronchoalveolar lavage fluid (BALF) was collected to detect cytokine levels as previously described.<sup>20</sup> After centrifugation at 3000g for 5 min, the supernatant of the BALF was harvested and preserved in refrigerator at  $-80^\circ\text{C}$  pending subsequent experiments. The ELISA assay kits (CUSABIO, Hubei, China) were exploited to measure IFN- $\gamma$ , IgE, IL-4, and IL-5 levels in the BALF from each group of mice. Then, the precipitate was resuspended to count total cells and different types of cells (macrophages, eosinophils, neutrophils and lymphocytes) by using a light microscope.

### Lung histology

After BALF samples were obtained, half of each left lung tissues in each group were quickly fixed in 4% paraformaldehyde at  $4^\circ\text{C}$  overnight prior to being embedded in paraffin, and the remaining tissues were frozen at  $-80^\circ\text{C}$  for subsequent experiment. Then, the paraffin-embedded tissues were sliced into 5  $\mu\text{m}$  thickness sections to undergo hematoxylin and eosin (H&E) staining. The inflammatory lesions of the lung tissue were observed under a light microscope and measured using Image-Pro Plus software (version 6.0). The inflamed area of lung tissue in H&E staining for quantification of lung changes was measured as previously described.<sup>21</sup>

### Protein digestion, TMT labeling, and enrichment of acetylated peptides

After the frozen lung tissues were fully pulverized in liquid nitrogen, the pulverized tissues were thoroughly mixed with chilled RIPA extraction buffer (Beyotime, Shanghai, China). After that, the mixture was sonicated, followed by centrifugation at 5000g for 3 min at 4°C. Next, the supernatant was harvested and mixed with 2 mM ethylenediaminetetraacetic acid (EDTA), 20 mM iodoacetamide, 10 mM dithiothreitol and protease inhibitor cocktails (Sigma-Aldrich, St. Louis, MO, USA). Five amounts of pre-cold acetone containing 10% (v/v) trichloroacetic acid were added and mixed well. After incubation for 2 h at 4°C, the mixture was subjected to centrifugation at 5000g at a constant temperature of 4°C to remove the supernatant. The precipitate was rinsed thrice with cold acetone, thawed in RIPA buffer, and air-dried at room temperature. After quantifying proteins by using a BCA kit (Thermo Fisher Scientific, Waltham, MA, USA), equal amount of total protein from each group was subsequently mixed with sequencing grade trypsin (Roche, Ingelheim, Germany) in accordance with a trypsin/protein ratio of 1/50 for incubation overnight at 37°C.

Then, desalting and drying of the digested peptides were carried out by means of Strata X C18 (Phenomenex) and vacuum centrifugation, respectively. Next, 0.5 M triethyl-ammonium bicarbonate buffer was used to dissolve the peptides before the labeling reagent (TMT-6plex™ Isobaric Label Reagent (TMT126-131) (ThermoFisher, CA, USA) was added according to the recommended protocol. TMT reagent was prepared by dissolution in anhydrous acetonitrile (ACN). After incubation at 25°C for 2 h, the reaction was quenched by adding hydroxylamine (8 µL of 5%) and subsequently incubated for 15 min.

The procedure of peptides enrichment was as follows: tryptic peptides were melted in NETN buffer (pH 8.0) containing 100 mM NaCl, 50 mM Tris-HCl, 1 mM EDTA, and 0.5% NP-40 prior to incubation with pre-washed antibody beads (PTM Biolabs, Hangzhou, China) in shaker-incubator at 4°C overnight. After the beads were rinsed thrice with NETN buffer and twice with ddH<sub>2</sub>O, bound peptides were eluted and collected from the beads with 0.1% trifluoroacetic acid, followed by vacuum-dried, and purified with C18 ZipTips (Millipore, Billerica, MA, USA).

### Peptide fractionation and liquid chromatography tandem-mass spectrometry analysis

Peptides were used to perform high pH fractionation by using an Agilent 300 Extend C18 chromatographic column (5 mm particles, 4.6 mm ID, 250 mm length) through the reversed phase liquid chromatography. Buffer A consisted of 98% H<sub>2</sub>O and 2% ACN, while buffer B contained 98% ACN and 10% H<sub>2</sub>O. Both the buffers contained 10 mM ammonium formate. The gradient program for elution of peptides was as follows: 2%–5% buffer B for 5 min, 5%–8% buffer B for 5 min, 8%–18% buffer B for 25 min, 18%–32% buffer B for 22 min,

32%–95% buffer B for 2 min, 95% buffer B for 4 min, and 95%–5% buffer B for 4 min. From the 16th min to 74th min, fractions were taken every minute. A total of 58 fractions were harvested and pooled into 18 fractions using concatenation scheme (1 + 19 + 37 + 55, 2 + 20 + 38 + 56, etc.). The flow rate of the program was 300 µl/min. Pooled fractions were subsequently desalted and lyophilized for further LC-MS/MS analysis.

Next, by using a nano-ultra-high-performance liquid chromatography EASY-nLC 1000 system (Thermo Fisher Scientific), each pooled fraction dissolved in 0.1% formic acid (FA) was performed on a reverse phase nanospray column at a flow rate of 350 nl/min. An elution system comprising buffer A (2% ACN in 0.1% FA) and buffer B (98% ACN in 0.1% FA) was applied to elute the peptides with a linear gradient of 7%–80% over 40 min. The parameters of the instrument were set as follows: electrospray voltage = 2.0 kV; m/z scan range = 350–1800 for a full scan; resolution in the Orbitrap for detection of intact peptides/fragments = 70,000/17,500; automatic gain control = 5000; fixed first mass = 100 m/z, and dynamic exclusion = 15.0 s.

### Data processing and database searching

All RAW files were processed using MaxQuant software (Version 1.4.1.2, Germany) against the UniProt\_Mus database. For protein identification, acetylation of lysine and protein N-termini, and oxidation of methionine were selected as variable modifications, while the carbamidomethylation of cysteine residues was selected as fixed modification. The search parameters were: Peptide mass tolerance = 10 ppm; missed cleavage = 4; MS/MS tolerance = 0.02 Da; Enzyme = Trypsin/P; Fixed modification = carbamidomethylation of cysteine residues; Variable modification = acetylation of lysine and protein N-termini; and oxidation of methionine. A false discovery rate ≤ 1% was selected as the threshold of these data for protein identification.

### Validation of MS result with Western blotting

Western blot analysis was conducted as in a previous study by Safavi *et al.*<sup>22</sup> The lung tissues from each group were lysed using a RIPA buffer. After centrifugation, the protein was quantified with a BCA protein assay kit (Beyotime, Shanghai, China). An equal amount of protein from each group was separated by 10% SDS-PAGE and subsequently transferred onto PVDF membranes. Next, the membrane was blocked with 5% skimmed milk for 2 h at 25°C, and incubated later with primary antibodies (H3K9ac, H3K14ac, H3K18ac, H3K27ac, and H3K36ac) (1:1000) overnight at 4°C. After that, the membranes were incubated with secondary antibodies for 1 h at 25°C. The membranes were rinsed thrice with TBST solution before each incubation with antibodies. Immunoreactive proteins were visualized by using ECL Plus reagent (Solarbio, Beijing, China). Expression of proteins was quantified using a UVP gel imaging system (Bio-Rad, USA) and analyzed using Gel-Pro analyzer.



## Immunohistochemical staining of lung tissue sections

Lung sections from each group were baked for 1 h at 70°C before deparaffinization and hydration. Then, normal goat serum was applied to conduct antigen retrieval and blockage for the sections. The sections were successively incubated with specific primary antibodies (1:50), biotinylated goat anti-mouse/rabbit IgG polymer, and streptavidin working solution labeled with horseradish peroxidase isozyme. Afterward, these sections were stained with diaminobenzidine and hematoxylin, dehydrated with gradient alcohol and mounted with neutral balsam. Finally, by counterstaining the lung tissue slides with DAB Substrate Kit (Thermo Scientific), the localization of histone acetylation sites including H2BK5ac, H2BK11ac, H2BK16ac, H2BK20ac, H2BK116ac, H2BK120ac, H3K9ac, H3K14ac, H3K18ac, H3K27ac, and H3K36ac were observed.

## Statistical analysis

The experiments were done at least thrice. All the results were presented as average  $\pm$  SD (standard deviation). In this study, all statistical analyses were performed and graphs were plotted by using GraphPad Prism Software, Version 7.0 for Windows (GraphPad Software Inc., San Diego, CA, USA). Between-group comparisons of the

results were made by *t*-test. The discrepancy was considered statistically significant at  $P < 0.05$ .

## Results

### Establishment of chronic asthma mouse model

First of all, our study generated an allergic airway inflammation model to mimic asthma. The pulmonary function test result showed that the airway responsiveness of the model group significantly increased after 8 weeks of OVA atomization compared to the normal control group ( $P < 0.05$ ) (Figure 1(A)). Besides, the concentration of IL-4, IL-5, IFN- $\gamma$ , and IgE levels in the BALF was measured by using ELISA. As shown in Figure 1(B), compared to the control group, the model group had obviously higher IL-4, IL-5, IgE levels and significantly lower IFN- $\gamma$  levels ( $P < 0.05$ ) (Figure 1(B)). As depicted in Figure 1(C), the number of each type of cells (macrophages, eosinophils, neutrophils, and lymphocytes) in BALF was significantly lower in the control group compared with the model group (all  $P < 0.05$ ). We further investigated the inflammatory extent of the lung tissues by H&E staining. In the model group, infiltration of inflammatory cells including eosinophils and neutrophils, was observed surrounding the peribronchial and perivascular areas, as well as blood vessels. We also found the exfoliated airway epithelium, and the

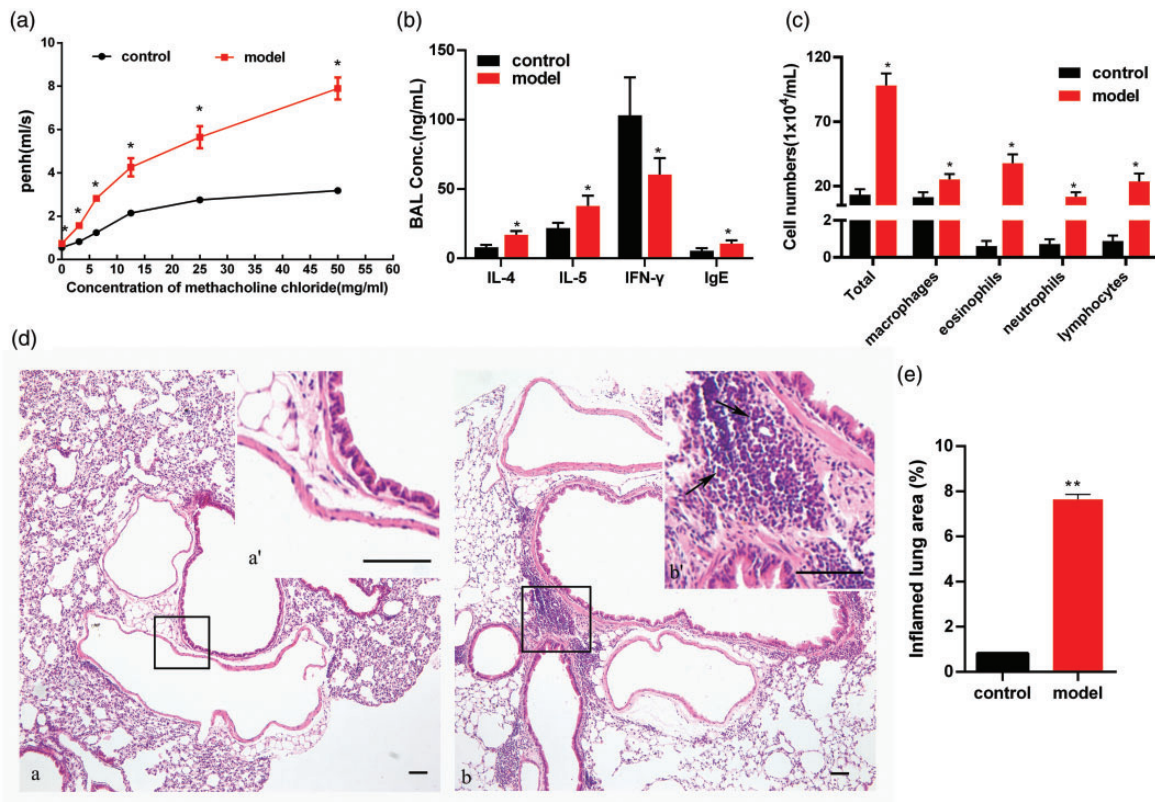


**Figure 1.** Establishment of chronic asthma mouse model. (a) Mice inhaled increasing doses of acetyl- $\beta$ -methylcholine chloride (3.125–50 mg/ml), and AHR was measured. (b) The total and differentiated cell count in the BALF. (c) Cytokines (IL-4, IL-5, and IFN- $\gamma$ ) and IgE concentration in the BALF. (d) The images of lung sections with H&E staining (scale bar, 50  $\mu$ m) and (e) the percentage of inflamed lung area are shown. Note: (a) and (b) represented lung sections of the control and the model groups, respectively; (a') and (b') respectively represented magnification views of the box in (a) and (b). Compared to the asthma group, \* $P < 0.05$ . (A color version of this figure is available in the online journal.) BAL: bronchoalveolar lavage.

thickened airway smooth muscle and alveolar septum in the sections from model group (Figure 1(D)). Moreover, the percentage area of inflammatory infiltration in the model group was pointedly enlarged when compared with the control group (Figure 1(E)). These results suggested that the allergic asthma model was successfully established.

### Quantitative proteomic profiling of histone acetylation in lungs of allergic asthma model

Through the iTRAQ analysis, proteins from mice lungs with or without asthma were identified. Then the specific acetyl lysine antibodies were employed to enrich acetylated peptides, and the peptides were analyzed by LC-MS/MS (Figure 2(A)). A total of 581 acetylation sites in 335 proteins were identified, and 351 acetylation sites in 215 proteins were quantified. The acetylation site was considered to be significantly changed when its quantitative ratio between two groups was more than 1.2. We found that 35 acetylation sites were upregulated, and 33 acetylation sites were downregulated in lungs of the allergic asthma model mice (Table 1). In addition, we obtained a total of 39 histone acetylation sites in the identified 351 acetylation sites, and 15 of these sites were obviously changed in the model group compared with the control. Among the 15 differential histone acetylation sites, 13 histone acetylation sites (H2B1C: K16, K20, K108, K116, K120; H2B1K: K120; H2B2B: K20; H3: K9, K14, K18, K23, K27, K36) were upregulated while two (H2B1C: K5, K11) were downregulated (Figure 2(B)). The changed acetylation sites were mainly located in H2B and H3 histone, while the acetylation sites in H1, H2A, and H4 were hardly changed (Figure 2(B)).

### Western blot validation of histone acetylation site

The relative contents of H3K9ac, H3K14ac, H3K18ac, H3K27ac, and H3K36ac were detected by western blot to validate the results of the iTRAQ analysis. The result is depicted in Figure 3 and showed that the levels of acetylation in H3K9, H3K14, H3K18, H3K27, and H3K36 sites of H3 histone from the model group were remarkably higher than those from the control group ( $P < 0.05$ ). Such results showed the same tendency with the results of the iTRAQ analysis. In addition, the result of western blotting showed a more significant difference of histone acetylation between both groups.

### Distribution of differentially modified acetylation sites in the lung tissue of asthmatic mice

To further clarify the role of the differentially expressed histone acetylation sites in the pathogenesis of asthma, we further analyzed the expression patterns of the

**Table 1.** The result for identification of acetylation sites in lung tissues.

Type of protein	Total number of sites	Changed sites	Upregulated sites	Downregulated sites
Total	351	68	35	33
Histone	39	15	13	2
Histone 1 (H1)	1	0	0	0
Histone 2A (H2A)	2	0	0	0
Histone 2B (H2B)	19	9	7	2
Histone 3 (H3)	10	6	6	0
Histone 4 (H4)	7	0	0	0

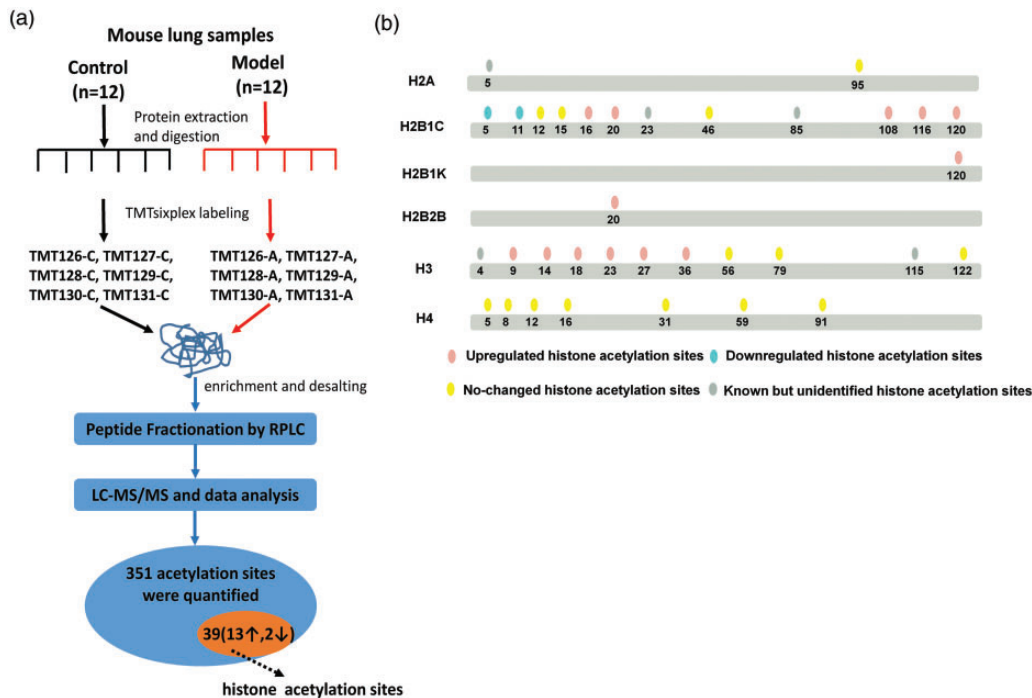


**Figure 2.** Quantitative proteomic profiling of histone acetylation in lungs of allergic asthma model. (a) Workflow of quantitative proteomics analysis of histone acetylation in lung tissues of normal and asthmatic mice. (b) Changes and distribution of histone acetylation sites. (A color version of this figure is available in the online journal.)

LC-MS/MS: liquid chromatography tandem-mass spectrometry; RPLC: reversed phase liquid chromatography; TMT: tandem mass tag.

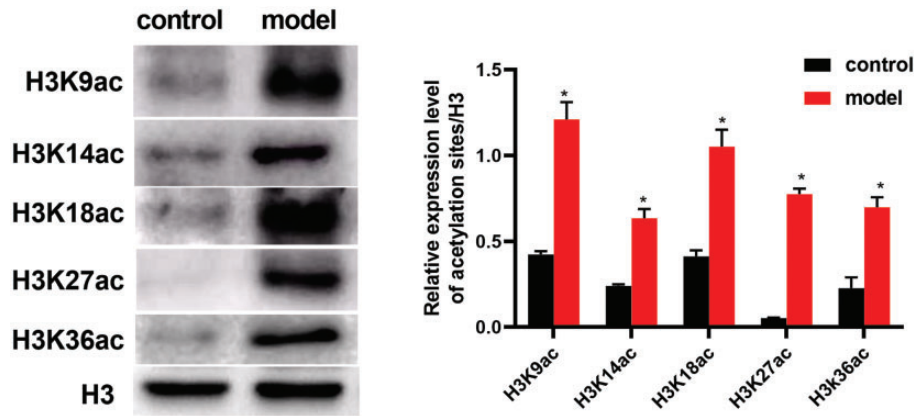


**Figure 3.** Verification of identified histone acetylation sites. The acetylation sites H3K9ac, H3K14ac, H3K18ac, H3K27ac, and H3K36ac were verified by performing western blot experiments for detection of protein expression. Note: Compared to asthma group, \* $P < 0.05$ . (A color version of this figure is available in the online journal.)

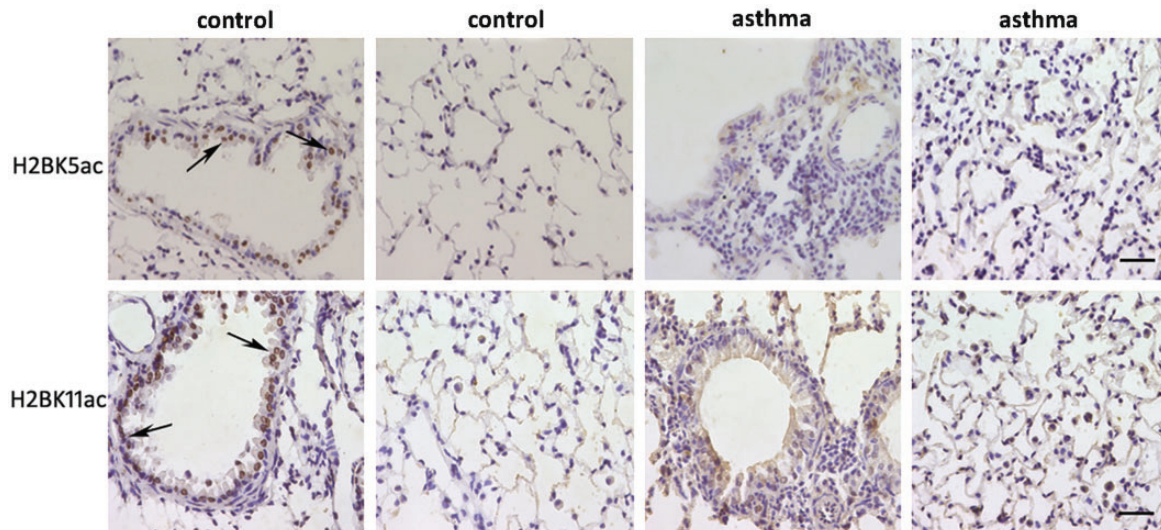


**Figure 4.** Expression of H2BK5ac and H2BK11ac in the lung tissue. Arrows indicate airway epithelial cell. (A color version of this figure is available in the online journal.)

identified acetylation sites which included H2BK5ac, H2BK11ac, H2BK16ac, H2BK20ac, H2BK116ac, H2BK120ac, H3K9ac, H3K14ac, H3K18ac, H3K27ac, and H3K36ac by IHC staining. As shown in Figure 4, the expressions of H2BK5ac and H2BK11ac in airway epithelial cells of normal mice were significantly higher than those of asthmatic mice. Whether in the normal or model group, the expression levels of H2BK5ac and H2BK11ac were extremely low in alveolar cells (Figure 4). Besides, H2BK20ac, H2BK116ac, H2BK120ac, H3K9ac, H3K18ac, H3K27ac, and H3K36ac were rarely expressed in lung tissues of normal group, but showed high expression levels in lung tissues of the model group. We found that the distribution of the above overexpressed histone acetylation sites in the lung tissues was not identical. As depicted in Figure 5, H2BK20ac, H2BK120ac, and H3K18ac were highly expressed in the nucleus of airway epithelial cells, while H2BK116ac were highly expressed in airway epithelial and vascular smooth muscle cells. Additionally, H3K27ac was highly expressed in alveolar macrophages and eosinophils, and H3K9ac and H3K36ac were highly expressed in

airway epithelial cells, alveolar macrophages, and eosinophils. Notably, the expression of H2BK16ac and H3K14ac in the lung tissue was more widespread, mainly in airway epithelial cells, alveolar macrophages, eosinophils, perivascular inflammatory cells and airways and vascular smooth muscle cells (Figures 6 and 7). The distribution of various histone acetylation expressions has been summarized in Table 2.

## Discussion

Asthma is an airway inflammatory disorder regarding various cells including airway epithelial cells, eosinophils, and neutrophils during its pathogenesis. Epidemiological research showed that asthma is affected by environmental, genetic as well as epigenetics factors, which suggested that no single genetic mutation will be causative. It is known that the central factor of asthma is immunological response to environmental stimuli. Multiple previous studies showed that activation of multiple inflammatory genes and overexpression of inflammatory protein eventually



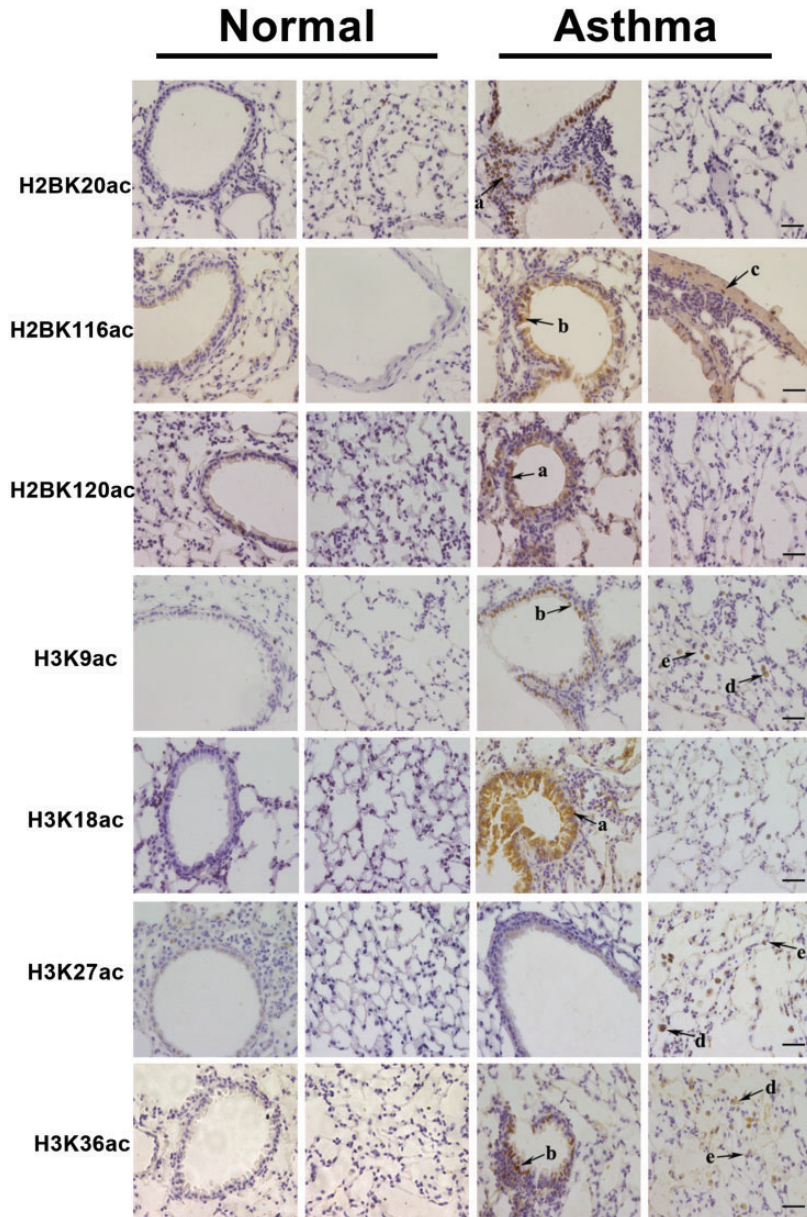


**Figure 5.** Expression and localization of H2BK20ac, H2BK116ac, H2BK120ac, H3K9ac, H3K18ac, H3K27ac, and H3K36ac in the lung tissues. (a) nucleus of airway epithelial cell; (b) airway epithelial cells; (c) vascular smooth muscle cell; (d) macrophage; (e) eosinophil. (A color version of this figure is available in the online journal.)

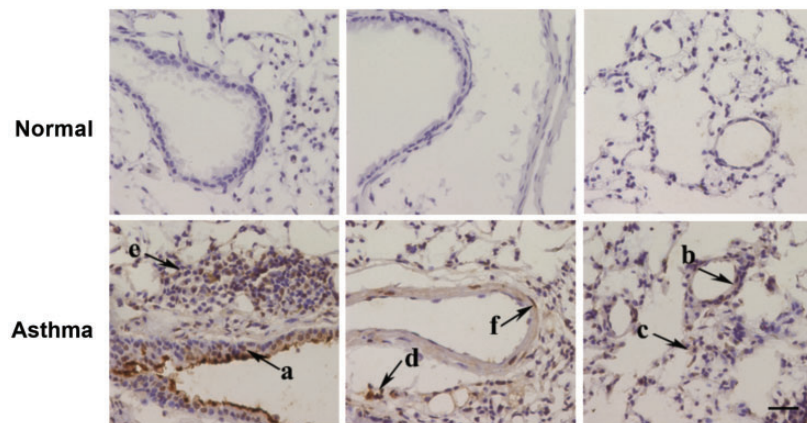


**Figure 6.** Expression and localization of H2BK16ac in the lung tissue. (a) Airway epithelial cells; (b) vascular smooth muscle cells; (c) macrophage; (d) eosinophil; (e) perivascular inflammatory cell; (f) airway smooth muscle cell. (A color version of this figure is available in the online journal.)

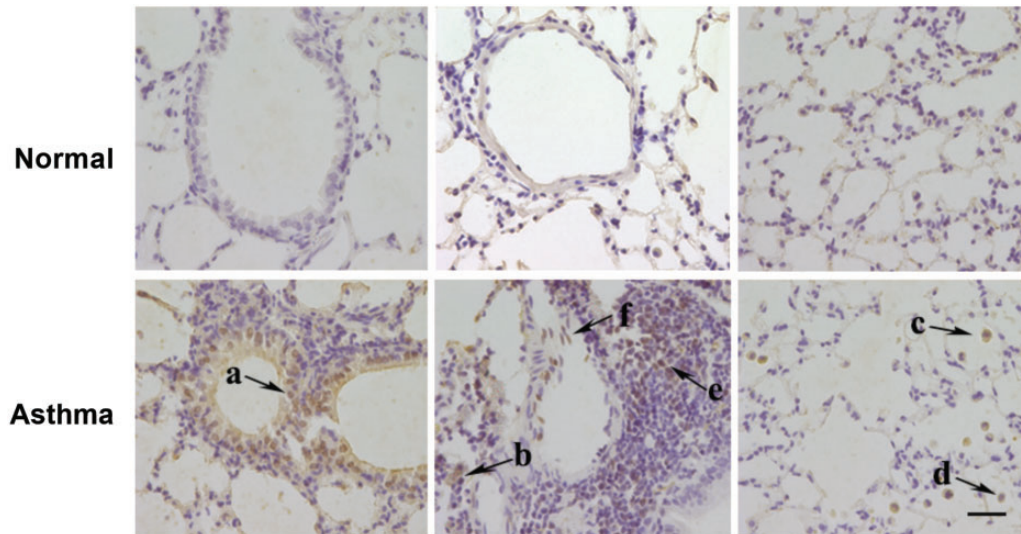


**Figure 7.** Expression and localization of H3K14ac in the lung tissue. (a) airway epithelial cells; (b) vascular smooth muscle cells; (c) macrophage; (d) eosinophil; (e): perivascular inflammatory cell; (f) airway smooth muscle cell. (A color version of this figure is available in the online journal.)

lead to a series of asthma symptoms.<sup>23,24</sup> Therefore, gaining greater insight into the cause of immune deviation and the function of epigenetics in asthma is crucial. The acetylation of histones plays an important role in chromatin remodeling and gene expression. There are many potential acetylation sites in the nucleosome octamers composed of histones H2A, H2B, H3, and H4. As reported, the acetylation sites are mainly distributed in H3 and H4, followed by H2A and H2B.<sup>25–27</sup> In a previous study of Scott's group, researchers found that histone ratio of deacetylase and histone acetyltransferase is relative to the severity of atopic asthmatic children's bronchial hyper-responsiveness,<sup>28</sup> which hinted the potential role of histone acetylation in asthma pathogenesis.

In this study, we established allergic airway inflammation model to mimic asthma according to previously described methods.<sup>11</sup> Not only the IL-4, IL-5, and IgE levels, but also the number of eosinophils in BALF of allergic airway inflammation model was observably increased when compared with that of normal mice. The combination of these results with those of HE staining suggested that the model was successfully established. Based on this, the combination of TMT labeling method with tandem mass spectrometry was applied to identify the differential expressed acetylation sites between the control and model groups. Initially, 581 acetylation sites in proteins were identified, then 351 of them were quantified which included 39 histone acetylation sites. After that, we found that a total of 15 differential expressed histone acetylation sites which included H3K9ac, H3K14ac, H3K18ac, H3K23ac, H3K27ac, H3K36ac, H2BK5ac, H2BK11ac, H2BK16ac, H2BK20ac, H2BK108ac, H2BK116ac, H2B1KK120ac, H2B2BK20ac, and H2BK120ac. As outlined above, all of the identified differentially modified acetylation sites were in histone H2B and H3, suggesting that histone acetylation in asthma occurred mainly in H2B and H3 rather than other histones. Several studies revealed that the changes of H3K9ac and H3K27ac were associated with air pollution that induced respiratory

disorders.<sup>29,30</sup> A previous study conducted by Cui *et al.* indicated that the acetylation levels of H3K9ac, H3K14ac, H3K27ac, and H3K18ac were obviously elevated in asthmatic lung tissues compared to the control group,<sup>31</sup> which corroborated with our finding. Studies elucidating the roles of histone H2B in asthma are limited. Despite the correlation of H2BK5ac and asthma has not been demonstrated, recent data suggested that EMT is regulated by H2BK5ac,<sup>32,33</sup> thus we speculated that H2BK5ac participated in the pathogenesis of asthma via regulating EMT. Besides, H2BK20ac and H2BK120ac have been proven a strong correlation with DNA methylation,<sup>34</sup> which hinted that they may regulate gene expression to affect disease development.

Subsequently, western blotting was used to validate some of the differentially modified acetylation sites identified in proteomics analysis. After that, with the aim of exploring the role of identified acetylation sites, we performed IHC staining based on the lung tissues of the control and model groups. Surprisingly, the expressions of these identified acetylation sites were distributed differentially in lung tissue according to cell types. In airway epithelial cells, the expressions of H3K9ac, H3K14ac, H3K16ac, H3K36ac, and H2BK116 in the model group were significantly higher than the control group, while the expressions of H2BK5 and H2BK11 showed opposite result. In addition, the H3K9ac, H3K14ac, H3K16ac, H3K27ac, and H3K36ac were differentially expressed in alveolar macrophage. Some studies indicated that H3K9ac and H3K27ac were involved in the regulation of macrophage polarization,<sup>35–37</sup> which supported the results obtained in this work. We also found a similar situation in eosinophil. As a central factor in asthma pathogenesis, eosinophil could be used as a potential predictor of asthma exacerbation,<sup>38–40</sup> and a previous study revealed that histone hyperacetylation contributes to eosinophilic airway inflammation.<sup>41</sup> So we speculated that the high expressions of H3K9ac, H3K14ac, H3K16ac, H3K27ac, and H3K36ac in eosinophil may play



Table 2. Expression distribution of the identified histone acetylation sites.

Histone acetylation sites	Airway epithelial cells		Nucleus of airway epithelial cells		Vascular smooth muscle cells		Alveolar macrophage		Eosinophil		Perivascular inflammatory cells		Airway smooth muscle cells	
	Normal	Model	Normal	Model	Normal	Model	Normal	Model	Normal	Model	Normal	Model	Normal	Model
H2BK5														
H2BK11	+													
H3K18	+													
H2BK20														
H2BK120														
H2BK116		+				+								
H3K27														
H3K9														
H3K36														
H3K16														
H3K14														

a role in asthma exacerbation. Furthermore, the current study also found the expression of H3K18ac, H2BK20ac, and H2BK120ac in nucleus of airway epithelial cells. Similar to our result, Stefanowicz *et al.* demonstrated that airway epithelial cells of asthmatic patients exhibited an elevated H3K18 acetylation rate.<sup>12</sup> These findings indicated that the pathogenesis of asthma is related to various cells, and the differentially expressed acetylation site in these cells is likely to be associated with abnormal transcriptional activation in the pathogenesis of asthma. Nevertheless, more detailed studies need to be conducted in the future to better understand this phenomenon. Harb *et al.* revealed the strong associations of histone acetylation levels in IFNG, SH2B3, and HDAC4 genes with risk of allergic sensitization.<sup>42</sup> Abbring *et al.* explored the role of histone acetylation of Th2 genes by using the Chromatin Immunoprecipitation analysis.<sup>43</sup> Based on the data of our current study, we speculated the histone acetylation we identified might have interaction with epithelial and inflammatory genes involved in asthma development.

Our study is the first to identify potential differentially expressed histone acetylation sites associated with asthma and to explore the distribution of the identified histone acetylation sites in cells involved in asthma pathogenesis using iTRAQ combined with LC-MS/MS. However, there are some limitations in this study. First, we found that the level of some cytokines as well as the number of eosinophils in BALF of allergic airway inflammation model were significantly higher than those of normal mice, but the factors associated with significant expression of these cytokines lacked further exploration; since we found differentially expressed acetylation sites in this study, we plan to study the effects of these acetylation sites and other factors such as methylation and abnormal gene expression on the inflammatory cytokines in asthma in future studies. Second, although our study identified the histone acetylation sites associated with pathogenesis of asthma, which were mainly expressed in airway epithelial cell, alveolar macrophage and eosinophil, their mechanism on regulating cell functions or gene expression needs to be further explored. Future studies will focus on exploring the correlation of these identified histone acetylation sites and asthma-related genes, and confirming the regulatory role of these histone acetylation sites in different types of cells involved in asthma development.

In conclusion, we identified a total of 15 differentially expressed histone acetylation sites which included 13 upregulated sites (H3K9ac, H3K14ac, H3K18ac, H3K23ac, H3K27ac, H3K36ac, H2B1KK120ac, H2B2BK20ac, H2BK16ac, H2BK20ac, H2BK108ac, H2BK116ac, and H2BK120ac) and 2 downregulated sites (H2BK5ac and H2BK11ac), and preliminary explored their differential expression distribution in different cell types involved in asthma pathogenesis in the lung tissue. This study screened out the potential epigenetic target for asthma-related genes, which may provide a novel point to develop more specific epigenetic modifying agents for asthma treatment.

## AUTHORS' CONTRIBUTIONS

YR wrote the manuscript. ML, SB, and LK contributed to analysis and interpretation of data. SB and LK conducted the experiments and obtained the data. XS designed the study and revised the manuscript. All the authors have read and approved the final version of the submitted manuscript.

## DECLARATION OF CONFLICTING INTERESTS

The author(s) declared no potential conflicts of interest with respect to the research, authorship, and/or publication of this article.

## FUNDING

The author(s) disclosed receipt of the following financial support for the research, authorship, and/or publication of this article: This work was supported by the National Natural Science Foundation of China (grant number 81770021), the Natural Science Foundation of Liaoning Province (grant number 201701664) and the postdoctoral program (grant number 2018M641749).

## ORCID iD

Xinming Su  <https://orcid.org/0000-0003-0053-4793>

## REFERENCES

- Moffatt MF, Kabesch M, Liang L, Dixon AL, Strachan D, Heath S, Depner M, von Berg A, Bufe A, Rietschel E, Heinzmann A, Simma B, Frischer T, Willis-Owen SA, Wong KC, Illig T, Vogelberg C, Weiland SK, von Mutius E, Abecasis GR, Farrall M, Gut IG, Lathrop GM, Cookson WO. Genetic variants regulating ORMDL3 expression contribute to the risk of childhood asthma. *Nature* 2007;**448**:470-3
- Bannister AJ, Kouzarides T. Regulation of chromatin by histone modifications. *Cell Res* 2011;**21**:381-95
- Alaskhar Alhamwe B, Khalaila R, Wolf J, von Bülow V, Harb H, Alhamdan F, Hii CS, Prescott SL, Ferrante A, Renz H, Garn H, Potaczek DP. Histone modifications and their role in epigenetics of atopy and allergic diseases. *Allergy Asthma Clin Immunol* 2018;**14**:39
- Graff J, Tsai LH. Histone acetylation: molecular mnemonics on the chromatin. *Nat Rev Neurosci* 2013;**14**:97-111
- Kidd CD, Thompson PJ, Barrett L, Baltic S. Histone modifications and asthma. The interface of the epigenetic and genetic landscapes. *Am J Respir Cell Mol Biol* 2016;**54**:3-12
- Brook PO, Perry MM, Adcock IM, Durham AL. Epigenome-modifying tools in asthma. *Epigenomics* 2015;**7**:1017-32
- Potaczek DP, Harb H, Michel S, Alhamwe BA, Renz H, Tost J. Epigenetics and allergy: from basic mechanisms to clinical applications. *Epigenomics* 2017;**9**:539-71
- Royce SG, Dang W, Ververis K, De Sampayo N, El-Osta A, Tang ML, Karagiannis TC. Protective effects of valproic acid against airway hyperresponsiveness and airway remodeling in a mouse model of allergic airways disease. *Epigenetics* 2011;**6**:1463-70
- Choi JH, Oh SW, Kang MS, Kwon HJ, Oh GT, Kim DY. Trichostatin A attenuates airway inflammation in mouse asthma model. *Clin Exp Allergy* 2005;**35**:89-96
- Gunawardhana LP, Gibson PG, Simpson JL, Powell H, Baines KJ. Activity and expression of histone acetylases and deacetylases in inflammatory phenotypes of asthma. *Clin Exp Allergy* 2014;**44**:47-57
- Ren Y, Su X, Kong L, Li M, Zhao X, Yu N, Kang J. Therapeutic effects of histone deacetylase inhibitors in a murine asthma model. *Inflamm Res* 2016;**65**:995-1008
- Stefanowicz D, Lee JY, Lee K, Shaheen F, Koo HK, Booth S, Knight DA, Hackett TL. Elevated H3K18 acetylation in airway epithelial cells of asthmatic subjects. *Respir Res* 2015;**16**:95
- Seumois G, Chavez L, Gerasimova A, Lienhard M, Omran N, Kalinke L, Vedanayagam M, Ganesan AP, Chawla A, Djukanovic R, Ansel KM, Peters B, Rao A, Vijayanand P. Epigenomic analysis of primary human T cells reveals enhancers associated with TH2 memory cell differentiation and asthma susceptibility. *Nat Immunol* 2014;**15**:777-88
- Rout-Pitt N, Farrow N, Parsons D, Donnelley M. Epithelial mesenchymal transition (EMT): a universal process in lung diseases with implications for cystic fibrosis pathophysiology. *Respir Res* 2018;**19**:136
- Lee KY, Ito K, Hayashi R, Jazrawi EP, Barnes PJ, Adcock IM. NF-kappaB and activator protein 1 response elements and the role of histone modifications in IL-1beta-induced TGF-beta1 gene transcription. *J Immunol* 2006;**176**:603-15
- Unwin RD. Quantification of proteins by iTRAQ. In: Cutillas PR, Timms JF (eds) *LC-MS/MS in proteomics: methods and applications*. Totowa: Humana Press, 2010, pp. 205-15
- Wang J, Zhang J, Zhang CJ, Wong YK, Lim TK, Hua ZC, Liu B, Tannenbaum SR, Shen HM, Lin Q. In situ proteomic profiling of curcumin targets in HCT116 colon cancer cell line. *Sci Rep* 2016;**6**:22146
- Wang Z, Yu K, Tan H, Wu Z, Cho JH, Han X, Sun H, Beach TG, Peng J. 27-Plex tandem mass tag mass spectrometry for profiling brain proteome in Alzheimer's disease. *Anal Chem* 2020;**92**:7162-70
- Festing MF, Altman DG. Guidelines for the design and statistical analysis of experiments using laboratory animals. *ILAR J* 2002;**43**:244-58
- Ma Y, Zhang JX, Liu YN, Ge A, Gu H, Zha WJ, Zeng XN, Huang M. Caffeic acid phenethyl ester alleviates asthma by regulating the airway microenvironment via the ROS-responsive MAPK/Akt pathway. *Free Radic Biol Med* 2016;**101**:163-75
- van Zoelen MA, Wieland CW, van der Windt GJ, Florquin S, Nawroth PP, Bierhaus A, van der Poll T. Receptor for advanced glycation end products is protective during murine tuberculosis. *Mol Immunol* 2012;**52**:183-9
- Safavi A, Kefayat A, Sotoodehnejadnematalahi F, Salehi M, Modarressi MH. Production, purification, and in vivo evaluation of a novel multi-epitope peptide vaccine consisted of immunodominant epitopes of SYCP1 and ACRBP antigens as a prophylactic melanoma vaccine. *Int Immunopharmacol* 2019;**76**:105872
- Poon AH, Eidelman DH, Martin JG, Laprise C, Hamid Q. Pathogenesis of severe asthma. *Clin Exp Allergy* 2012;**42**:625-37
- Kabesch M. Epigenetics in asthma and allergy. *Curr Opin Allergy Clin Immunol* 2014;**14**:62-8
- Kimura A, Horikoshi M. Tip60 acetylates six lysines of a specific class in core histones in vitro. *Genes Cells* 1998;**3**:789-800
- Verreault A, Kaufman PD, Kobayashi R, Stillman B. Nucleosomal DNA regulates the core-histone-binding subunit of the human Hat1 acetyltransferase. *Curr Biol* 1998;**8**:96-108
- Marushige K. Activation of chromatin by acetylation of histone side chains. *Proc Natl Acad Sci U S A* 1976;**73**:3937-41
- Weiss ST, Van Natta ML, Zeiger RS. Relationship between increased airway responsiveness and asthma severity in the childhood asthma management program. *Am J Respir Crit Care Med* 2000;**162**:50-6
- Ding R, Jin Y, Liu X, Ye H, Zhu Z, Zhang Y, Wang T, Xu Y. Dose- and time-effect responses of DNA methylation and histone H3K9 acetylation changes induced by traffic-related air pollution. *Sci Rep* 2017;**7**:43737
- Leclercq B, Platel A, Antherieu S, Alleman LY, Hardy EM, Perdrix E, Grova N, Riffault V, Appenzeller BM, Hapillon M, Nesslany F, Coddeville P, Lo-Guidice JM, Garçon G. Genetic and epigenetic alterations in normal and sensitive COPD-diseased human bronchial epithelial cells repeatedly exposed to air pollution-derived PM(2.5). *Environ Pollut* 2017;**230**:163-77
- Cui ZL, Gu W, Ding T, Peng XH, Chen X, Luan CY, Han RC, Xu WG, Guo XJ. Histone modifications of Notch1 promoter affect lung CD4+ T cell differentiation in asthmatic rats. *Int J Immunopathol Pharmacol* 2013;**26**:371-81
- Mobley RJ, Raghu D, Duke LD, Abell-Hart K, Zawistowski JS, Lutz K, Gomez SM, Roy S, Homayouni R, Johnson GL, Abell AN. MAP3K4

- controls the chromatin modifier HDAC6 during trophoblast stem cell epithelial-to-mesenchymal transition. *Cell Rep* 2017;**18**:2387–400
33. Chitsazian F, Sadeghi M, Elahi E. Confident gene activity prediction based on single histone modification H2BK5ac in human cell lines. *BMC Bioinformatics* 2017;**18**:67
  34. Linghu C, Zheng H, Zhang L, Zhang J. Discovering common combinatorial histone modification patterns in the human genome. *Gene* 2013;**518**:171–8
  35. Iwanowycz S, Wang J, Altomare D, Hui Y, Fan D. Emodin bidirectionally modulates macrophage polarization and epigenetically regulates macrophage memory. *J Biol Chem* 2016;**291**:11491–503
  36. Theiler A, Barnthaler T, Platzer W, Richtig G, Peinhaupt M, Rittchen S, Kargl J, Ulven T, Marsh LM, Marsche G, Schuligoi R, Sturm EM, Heinemann A. Butyrate ameliorates allergic airway inflammation by limiting eosinophil trafficking and survival. *J Allergy Clin Immunol* 2019;**144**:764–76
  37. Czimmerer Z, Daniel B, Horvath A, Ruckerl D, Nagy G, Kiss M, Peloquin M, Budai MM, Cuaranta-Monroy I, Simandi Z, Steiner L, Nagy B Jr., Poliska S, Banko C, Bacso Z, Schulman IG, Sauer S, Deleuze JF, Allen JE, Benko S, Nagy L. The transcription factor STAT6 mediates direct repression of inflammatory enhancers and limits activation of alternatively polarized macrophages. *Immunity* 2018;**48**:75–90.e6
  38. Bergantini L, d'Alessandro M, Cameli P, Bianchi F, Sestini P, Bargagli E, Refini RM. Personalized approach of severe eosinophilic asthma patients treated with mepolizumab and benralizumab. *Int Arch Allergy Immunol* 2020;**181**:746–53
  39. Thomson NC. Novel therapies targeting eosinophilic inflammation in asthma. *Clin Exp Allergy* 2014;**44**:462–8
  40. Varricchi G, Marone G, Spadaro G, Russo M, Granata F, Genovese A, Marone G. Novel biological therapies in severe asthma: targeting the right trait. *Curr Med Chem* 2019;**26**:2801–22
  41. Zhang HP, Wang L, Fu JJ, Fan T, Wang ZL, Wang G. Association between histone hyperacetylation status in memory T lymphocytes and allergen-induced eosinophilic airway inflammation. *Respirology* 2016;**21**:850–7
  42. Harb H, Alashkar Alhamwe B, Acevedo N, Frumento P, Johansson C, Eick L, Papadogiannakis N, Alm J, Renz H, Potaczek DP, Scheynius A. Epigenetic modifications in placenta are associated with the child's sensitization to allergens. *Biomed Res Int* 2019;**2019**:1315257
  43. Abbring S, Wolf J, Ayechu-Muruzabal V, Diks MAP, Alhamwe BA, Alhamdan F, Harb H, Renz H, Garn H, Garssen J, Potaczek DP, van Esch B. Raw cow's milk reduces allergic symptoms in a murine model for food Allergy-A potential role for epigenetic modifications. *Nutrients* 2019;**11**:1721

(Received August 28, 2020, Accepted November 21, 2020)